Contents

7. Dynamic Modeling of Spacecraft in a Collisionless Plasma

Irá Katz, Donald E. Parks, Sang Wang, and Andrew Wilson
Plasma Physics Group
Systems, Science and Software
La Jolla, California

1. INTRODUCTION

Environmental charging of geosynchronous spacecraft to potentials of thousands of volts has been experimentally observed. Previous attempts to model spacecraft charging have employed techniques which are limited to simplified geometries and symmetry assumptions. In this paper, we describe a new computational model which can simulate the charging of complex geometrical objects in three dimensions. We present two sample calculations. In the first problem, the capacitance to infinity of a complex object similar to a satellite with solar array paddles is calculated. The second problem concerns the dynamical charging of a conducting cube partially covered with a thin dielectric film. In this calculation, the photoemission results in differential charging of the object.

2. THEORY

The interaction of a satellite and the magnetosphere can be separated into two parts. The first is the particle deposition, charge transport, and electrical

properties associated with charged particles impinging upon the satellite. The second part is the self-consistent ambient and photoplasma interactions with the electric field. The field must satisfy boundary conditions on the satellite consistent with the charge deposited on the satellite. To solve both parts of this problem completely and self-consistently for general, ambient plasmas is a formidable task. Here, we shall be concerned only with a limited (albeit very important) range of plasma environments (a hot magnetosphere). As a result, certain approximations reduce the magnitude of the problem.

The timescales of phenomena which occur on a spacecraft in the magnetosphere range from nanoseconds to hours (Table 1). The lower end of this range is associated with effects such as the discharging of electrical circuit elements and electromagnetic wave phenomena. At the upper end of the range, slow variations in the magnetospheric environment are important. In this paper, we shall be concerned with the intermediate timescale range, from milliseconds to seconds. This range is determined by the charging time of the surface of a spacecraft by magnetospheric electron currents.

Table 1. Characteristic Times for Charged Spacecraft in the Magnetosphere

Phenomenon	Time
Breakdown in circuit elements	$\tau_B \sim 10^{-9} - 10^{-8}$ sec
Charging of bare conducting surface	$\tau_c \sim 10^{-3}$ sec
Differential charging of thin dielectric overlying conductor	$\tau_D \sim 1$ sec
Charge redistribution in a dielectric	$\tau_{RD} \gtrsim 100$ sec
Change in environmental conditions	$\tau_E \gtrsim 1$ to $\sim 10^3$ sec

Before entering upon the analysis of these phenomena, it is useful to set the scale of the various processes involved. These are listed in Table 2, and, in each case, the treatments which must be applied to describe the relevant field and particle phenomena are indicated. In the magnetosphere, the plasma sheath surrounding a spacecraft requires a particle description. This is necessary on account of the very long mean free paths and long Debye lengths λ_D which occur in these hot, diffuse plasmas. Electromagnetic treatments are needed only for describing effects such as transient surface current phenomena resulting from arcing excitations. Particle dynamics must be followed if sheath plasma

Table 2. Collisionless Satellite-Plasma Sheath Models. L is the Spacecraft Size, ω_p is the Plasma Frequency and λ_D is the Debye Length

Model	Fields	Particle Treatment	Timescale
1. Electromagnetic	Maxwell's equations	Dynamic	L/c $\sim 10^{-9}$ sec
2. Quasistatic	Poisson's equations ($L \ll c\omega_p^{-1}$)	Dynamic	ω_p^{-1} $\sim 10^{-5}$ sec
3. Equilibrium	(a) Poisson ($\lambda_D \sim L$) (b) Laplace ($\lambda_D \gg L$)	Static	$\tau_c < t < \tau_D$ $>10^{-3}$ sec

oscillatory behavior is important.[1,2] On a longer timescale, the plasma is characterized by an equilibrium-particle distribution.[3,4] This is the range which is considered here. Finally, at the longest timescale, the behavior is determined by changes in the environment or redistribution of charges within dielectrics.

We shall now describe the considerations underlying our analysis of the intermediate timescale phenomena. Let us consider a spacecraft with a spherical conducting surface. With a radius R (cm) and a charging current density j (A/cm^2), the time taken to charge the spacecraft to a potential V is

$$\tau_c = \frac{C_\infty V}{4\pi R^2 j}$$

where C_∞ is the capacitance of the spacecraft with respect to infinity, and is given by

$$C_\infty = R \quad \text{esu}$$
$$\simeq 10^{-12} R \ F \ .$$

With the following values

$$R = 100 \text{ cm}$$
$$V = 10^3 \text{ V}$$
$$j = 0.5 \times 10^{-9} \text{ A/cm}^2$$

the charging time is

$$\tau_c \simeq \frac{10^{-12} V}{4\pi R\, j}$$

$$\simeq 2 \times 10^{-3} \text{ sec} \quad .$$

However, on most spacecraft, large areas are not bare conductors, but are covered by thin, insulating dielectrics overlying conducting substrates. In these cases, the capacitance of the dielectric, C_D, is important, rather than the capacitance with respect to infinity. The dielectric capacitance is

$$C_D \simeq \frac{1}{4\pi d} \text{ esu/cm}^2$$

$$\sim \frac{10^{-12}}{4\pi d} \text{ F/cm}^2 \quad .$$

With a thickness of 40 mil ($d \sim 0.1$ cm), the charging time τ_D is now

$$\tau_D \sim \frac{10^{-12} V}{4\pi d\, j} \sim \frac{10^{-9}}{1.2 \times 0.5 \times 10^{-9}}$$

$$\sim 1.6 \text{ sec} \quad .$$

The voltage buildup between a conductor and a dielectric insulator thus occurs very much more slowly than the buildup on a bare conductor. As a result, differential charging of a spacecraft takes place on a timescale longer than charging. Later, we shall describe the development of such a phenomenon over the timescale range $\tau_C < t \lesssim \tau_D$.

Under the conditions found in magnetospheric substorms, essential simplifications can be made in the modeling of the charging. In particular, we demonstrate below for hot, low density plasmas where

$$\lambda_D \gg L,$$

λ_D is the Debye length and L a characteristic object dimension, that if surface potentials on the satellite are of the order of the plasma temperature, one makes only a very small error by neglecting the ambient space charge density in Poisson's equation. This approximation, when justified, greatly reduces the amount of computation necessary to determine satellite potentials.

Let us examine the effect of a large ambient charge density fluctuation in a $\theta = 10$ keV, $n_e = 10\ cm^{-3}$ magnetospheric plasma. The Debye length of such a plasma is given by

$$\lambda_D \simeq 743\sqrt{\frac{\theta}{n_e}} \simeq 2 \times 10^4 \text{ cm}$$
$$= 200 \text{ m.}$$

It has been shown[5] that in equilibrium plasmas, maximum charge variations are of order of the ambient charge density. It follows then that the magnitude of a potential associated with a spherical charge density fluctuation of 1 m in radius is at most

$$\phi \sim \frac{q}{r} = \frac{4}{3}\pi r^2 n_e e \quad \text{esu}$$
$$= \frac{4}{3}\pi \cdot 10^4 \times 10 \times 4.8 \times 10^{-10}$$
$$\sim 2 \times 10^{-4} \text{ statvolts}$$
$$\sim 6 \times 10^{-2} \text{ volts}$$

which is several orders of magnitude less than the satellite surface potentials.

Another useful quantity to examine is the relative amount of charge on a sphere of a meter radius charged up to the ambient temperature to the amount of space charge such a volume would contain. The surface charge on a sphere of radius r is

$$q_{surface} = r\phi \simeq \frac{r\theta}{e} .$$

The space charge in such a plasma is

$$q_{plasma} = \frac{4}{3}\pi r^3 n_e e .$$

The ratio of these two charges is

$$\frac{q_{plasma}}{q_{surface}} = \frac{4}{3}\pi r^2 n_e \frac{e^2}{\theta} = \frac{1}{3}\left(\frac{r}{\lambda_D}\right)^2$$
$$< 10^{-5} .$$

Thus, we have strong reasons to believe that the gross potential features surrounding an object whose dimensions are much smaller than a Debye length and whose surface potentials are comparable to the plasma temperature can be calculated ignoring ambient (as distinct from photosheath) space charge effects.

3. NUMERICAL TECHNIQUES

The dynamical model consists of two parts, namely: (1) the calculation of surface charge densities and net charging currents, given a potential distribution, and (2) the calculation of the potential subject to free space and appropriate satellite boundary conditions. Brief descriptions of the techniques used are given below. Further details will be presented at a later date.

3.1 Surface Charging Calculation

We require the incident and outgoing currents $\vec{j}_{in}$, $\vec{j}_{out}$, respectively at surface points $\vec{r} = \vec{r}_o$. The net charging current is then

$$\vec{j}_{net}(\vec{r}_o) = \vec{j}_{in}(\vec{r}_o) - \vec{j}_{out}(\vec{r}_o)$$

where

$$\vec{j}_{in}(\vec{r}_o) = \int d^3 v_o \, \vec{v}_o \, f_{in}(\vec{v}_o, \vec{r}_o)$$

$$\vec{j}_{out}(\vec{r}_o) = \int d^3 v_o \, \vec{v}_o \, f_{out}(\vec{v}_o, \vec{r}_o) \quad .$$

The distribution f_{out} is assumed known at the surface $\vec{r} = \vec{r}_o$ and f_{in} is known at positions far away from the spacecraft. Since we are looking for equilibrium solutions of Vlasov's equation, the distribution functions satisfy

$$\frac{df}{dt} = 0$$

along particle trajectories. The object then is to calculate the trajectories of a selection of particles. Since we know the distribution function f far from the satellite, automatically we know the distribution, since f is constant along a given trajectory.

The Parker-Whipple[6] inside-out scheme makes use of this fact. Trajectories are initiated at the spacecraft surface and are traced backwards through the potential field to distant points where the distribution, $f(\vec{v})$ is known. One advantage

of this scheme is that orbits which do not have an endpoint on the spacecraft surface are avoided. The neglect of such orbits is strictly valid only if the volume spacecharge has no influence on the particle trajectories.

It should be emphasized that the machinery is contained in our numerical technique for calculating ambient charge densities by constructing distribution functions, f, in each spatial zone and taking its zeroth moment (as opposed to j, which is a first moment)

$$\rho = \int f \, d\vec{v}$$

However, presently, we do not calculate this term, based upon the arguments presented in Section 2.

3.2 Potential Calculation

In calculating the potential in three dimensions around an arbitrary object, a gridded method must be employed since the specification of the surface is far too general for analytical or multipole techniques. Since satellites are the order of meters in length, we need at least 10 cm resolution as an upper bound in the vicinity of the spacecraft. However, for determining particle orbits, the fields hundreds of meters away must also be known. In order to keep storage down to a reasonable level, some type of variable gridding must be employed. This precludes the use of any straightforward Fourier transform technique. One technique for achieving high resolution in the region around the object and still being able to handle vast quantities of space is through local mesh refinement. Finite difference approaches, however, have difficulty in mesh transition regions, especially when grid lines are terminated, and generally lose an order of accuracy in such regions.

As a result of this, we decided upon a finite element approach using right parallelepiped elements and blended linear univariate edge interpolants. This permits the same degree of accuracy over the entire mesh, even though the mesh elements differ in size. It results in the standard trilinear interpolation scheme for each element.

The fundamental approach is to solve Poisson's equation

$$\nabla^2 \phi = -4\pi\rho \tag{1}$$

by solving the associated variational principle

$$0 = \frac{\delta}{\delta\phi} \left\{ \int dV \, [(\nabla\phi)^2 + 4\pi\rho\phi] + \int d\vec{S} \cdot (4\pi\sigma + \nabla\phi)\phi \right\} \tag{2}$$

The first term in the integrand corresponds to the Laplacian operator. The second term is the volume spacecharge contribution. The remaining terms are surface contributions, referring to the surface charge and electric field, respectively.

In the variational calculation, we use locally defined basis sets, that is, trilinear interpolants within each cube-like element. Since the finite element equations are derived from Eq. (2), different mesh volumes automatically receive the correct variational weight. This ensures the maintenance of accuracy through mesh transition regions. The problem of local mesh refinement is approached by having grids within grids, that is, a chinese doll-like hierarchy of grids shown schematically in Figure 1. The theory of this technique is discussed in Birkhoff et al,[7] and Cavendish.[8] In order to have high computation speed, the linear equations resulting from the variational principle (Eq. (2)) in the interface region were coded up explicitly in a series of thirteen subroutines. These same routines are used for interfacing any pair of the meshes.

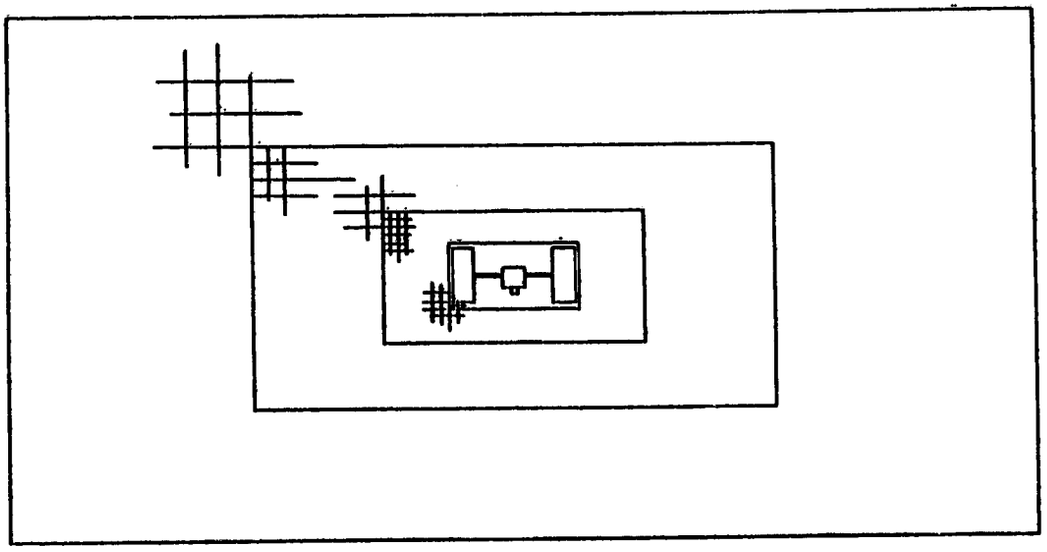

Figure 1. Cross-Section of Grid, Showing First Four Embedded Meshes

4. SAMPLE CALCULATIONS

To demonstrate the capabilities of our 3D model, we have performed two sample calculations. First, we calculated the capacitance, surface charge distribution and electric fields around a geometrically complex, conducting satellitelike object. The object is shown in Figure 2, and the problem was gridded as

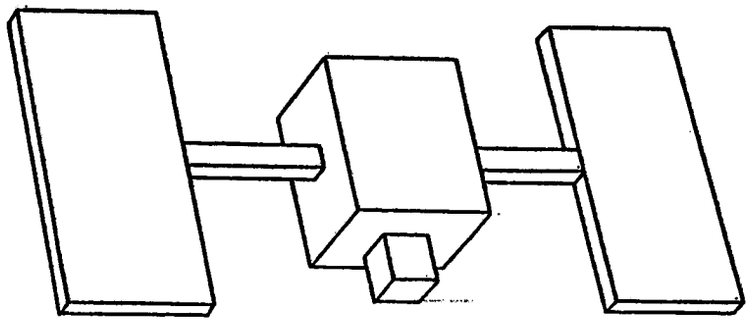

Figure 2. 3-D Model Spacecraft for Capacitance Calculation

shown in Figure 1. While it is electrically simple, being an equipotential surface, it has sufficient geometrical complexity to demonstrate some of the features of our TRILIN model. The overall length of the object is 6 m, with 20 cm resolution on the surface. The outermost grid is 51 m long, and there are about 30,000 variables in the problem. The outermost mesh had monopole ($\phi = \frac{q}{r}$) boundary conditions imposed. Using an SOR routine, this problem took less than 4 min to solve on the CDC 7600 at Kirtland Air Force Base.

The capacitance calculated for this object is 83 pF. The surface area of the object is almost four times as great as that of a sphere of equivalent capacitance (r = 75 cm). If placed in an environment with a charging current of 10^{-9} A/cm^2, this satellite-like object would charge to 10 keV in about 3 msec. The charge distribution is nonuniform, as expected, with most of the charge on the panels which have only 58 percent of the surface area. With the satellite charged to 10 kV, the total charge on the surface is approximately 2500 esu ($\sim 0.9\ \mu$C). The average normal electric fields on each panel in such a problem is ~ 37.5 V/cm while, on the body, it ranges from 20 V/cm to ~ 40 V/cm.

The second sample calculation is of a simpler geometry, but has considerable physical complexity. The object consists of a conducting cube, 60 cm on an edge, partially covered with a 1 mm insulation skin of dielectric constant unity. Figure 3 shows a picture of the object. The object is placed in a 10 keV, $n_e = 10$ cm^{-3} electron plasma with an assumed neutralizing background. By the backward trajectory technique described above, incident electron currents on the object are determined. Charge impinging upon the dielectric skin is assumed to stick while charge landing on the exposed conducting surfaces is allowed to distribute itself in order to maintain the conductor as an equipotential surface. The potential on dielectric surfaces is related to that on the conductor by the line integral of the electric field through the surface. To add asymmetry and cause differential charging, we assume a light source at some large distance along the

positive x-axis. This light gives rise to a photocurrent of 4 nA/cm^2 which acts to discharge that surface.

Initially the potential on the surface of the satellite rises very quickly. This corresponds to surface charging on a timescale determined by the net capacitance to infinity. However, after about 50 msec, the differential charging of the conductor and the front and back dielectric surfaces dominate the calculation. The potential at three locations as a function of time is plotted in Figure 4. We notice how the surface dielectric continues to charge, albeit at

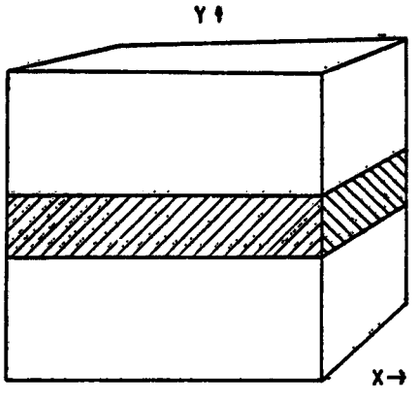

Figure 3. Spacecraft for Dynamical Calculation. Only dashed area is bare metal, the rest of the object is covered with a dielectric film

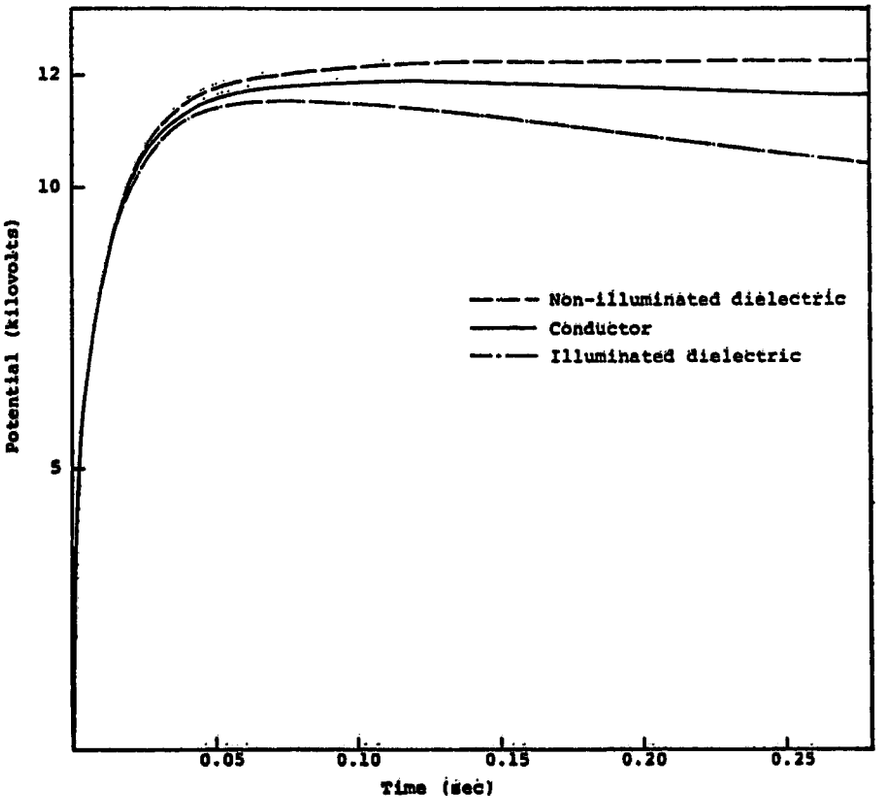

Figure 4. Comparison of Charge Buildup at Three Different Sections of Illuminated Spacecraft

a very slow rate, while the front surface dielectric discharges substantially. The conductor also discharged, but more slowly than the illuminated dielectric. Figure 5 shows a potential contour map through the x, y plane. We can see that the conductor is more than one thousand volts negative with respect to the front surface dielectric, while it is only a few hundred volts positive with respect to the rear surface dark dielectric. This implies that the conductors surface charge under the illuminated dielectric is of negative sign while underneath the rear dielectric the conductor's surface charge is of positive sign. The potential difference between front and rear dielectrics is almost two kilovolts. Fields in the front dielectric are greater than 10^4 volts/cm.

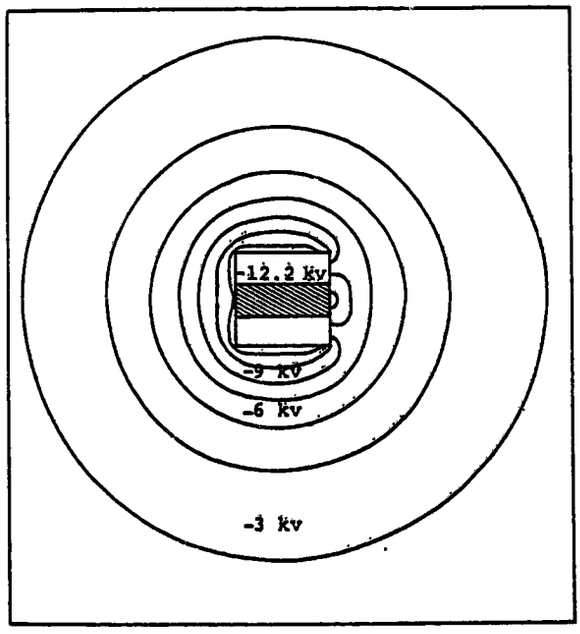

Figure 5. Potential Contour Plot Near the Spacecraft after 0.27 sec. Sunlight is incident from the right (x-direction)

5. CONCLUSIONS

The prediction of surface potentials on complex satellites is a formidable task. Material properties, geometrical effects, ambient plasma, and photosheath space charge all play roles in determining surface potential distributions.

However, for the range of plasma parameters frequently found in magnetospheric substorms, it is justifiable to neglect the self-consistent ambient plasma space charge. This assumption permits the calculation of potentials in asymmetric three-dimensional geometries. The resultant calculations demonstrate such effects as net object charging with respect to infinity, differential charging, and charge redistribution on conductors. These first calculations presented here employ large simplifications with respect to material properties, ion currents, etc. However, they show that the concept of three-dimensional spacecraft charging calculations is a practical one.

Acknowledgments

This work was supported by the Defense Nuclear Agency under Contract DNA001-76-C-0121 and by the National Aeronautics and Space Administration under Contract NAS3-20119.

References

1. Katz, I., Wilson, A., Parker, L.W., Rothwell, P.L., and Rubin, A.G. (1976) Static and dynamic behavior of spherical probe and satellite plasma sheaths, Conference on Nuclear and Space Radiation Effects, San Diego, July 1976 (to be published in IEEE Trans. on Nuclear Science, December, 1976).
2. Parks, D., Wilson, A., and Katz, I. (1976) Streaming instabilities in satellite plasma sheaths, Conference on Nuclear and Space Radiation Effects, San Diego, July 1976 (to be published in IEEE Trans. on Nuclear Science, December 1976).
3. Whipple, E.C., Jr. (1965) The Equilibrium Electric Potential of a Body in the Upper Atmosphere and in Interplanetary Space, NASA X-615-65-296, Goddard Space Flight Center, Greenbelt, Md.
4. Laframboise, J.G. (1966) UTIAS Report No. 100, University of Toronto, Canada.
5. Laframboise, J.G., and Parker, L.W. (1973) Phys. Fluids 16:629.
6. Parker, L.W. and Whipple, E.C., Jr. (1967) Ann. Phys. 44:126.
7. Birkhoff, G., Cavendish, J.C., and Gordon, W.J. (1974) Doc. Nat. Acad. Sci., USN 71:3423.
8. Cavendish, J.C. (1975) J. Comp. Phys. 19:211.